

Application of Plasma Focus Device for Nano-layers Deposition on Silicon Wafers¹

M. Chernyshova, L. Karpiński, M. Scholz, B. Ulejczyk, Jeon K. Lee*, Jae K. Lee*, and K. Jung*

Institute of Plasma Physics and Laser Microfusion, 23, Hery, Warszawa, 01-497 Poland

E-mail: lekarp@ifpilm.waw.pl

**Korean Institute of Science and Technology, P.O. Box 131, Cheongryang, Seoul, 130-650, Korea*

Abstract – In these studies, nano-layers were deposited at 50, 200 and 1000 mTr of pressure of argon-oxygen gas mixture. Silicon wafer, which was covered by nano-layer was placed 400 mm under an anode. Each nano-layer was deposited at the same number of shots. In the beginning four conditioning shots were performed. During these shots, a sample was screened by the shutter. Then the sample was unscreened and nano-layer was deposited at 10 shots. Nano-layers were investigated using scanning electron microscopy and Auger spectroscopy.

1. Introduction

Plasma Focus device (PF) has been successfully used as a pulsed ionizing radiation source for many applications: pulsed neutron activation analysis [1], as a high flux X-ray source for lithography and radiography [2–4], as highly energetic ion source for processing of materials in the form of thin films [5, 6] or surface modification [7, 8]. All the radiation is produced at the high-current discharge in a vacuum chamber filled with different gases at pressure of a few Tr. The sort of radiation depends on the type of gases inside the reactor, material of electrodes, geometry and other parameters [8]. For this reason, PF is very well fitted to a number of applications, in spite of the fact that a quite complicated picture of physical processes ruling a generation of radiation still is not understood completely.

In this work, we present the results of nano-layer deposition using the small PF device. The surface of nano-layers and their compositions are shown.

2. Experimental Set-up

This PF consists essentially of coaxial electrode assembly and an alumina insulator (Fig. 1) across which the initial breakdown occurs. The outer electrode (12 stainless-steel bars 12 mm in diameter) and center electrode (CE) diameter is 25 mm, with CE length of 80 mm. The minimum angular spacing, $\Delta r = 7$ mm, leads to uniform breakdown on the insulator and symmetrical current sheath propagation. The CE is connected to the collector linked electrically through the spark-gap switch arrangement to the capacitor

bank. The outer electrode (OE) is attached to a connection sleeve that provides vacuum seal. The cylindrical alumina insulator forms the vacuum seal between the connection sleeve and the collector. The central part of the insulator extends for about 3 cm along the CE into the vacuum chamber. Such an insulator arrangement prescribes the shape of the initial current sheath between the CE and the connection plate of the OE. The exposed insulator surface is minimized by such a geometry. A vacuum vessel of stainless steel surrounds the electrode system.

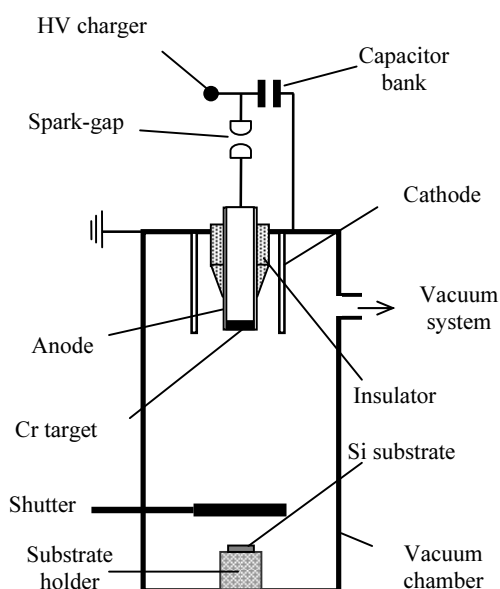


Fig. 1. Scheme of PF device

The CE (anode) is made of copper and a chromium target was mounted in the middle of the CE tip. Chromium target was used for film deposition. The OE and vacuum chamber were kept at ground potential. The films were deposited on Si wafers at room temperature mounted on the holder axially under the CE at the bottom of vacuum chamber. Distances between the Si wafer and the top of the CE were kept at 400 mm. The chamber was filled with gas mixture of argon and oxygen, 1:1.

Simple construction of the vacuum chamber does not allow us to put inside a sample without opening

¹ The work was supported by KIST.

the chamber and airing it. These operations, when the vacuum chamber is aired and opened, cause that insulator and electrode surfaces are changed under the air exposition. As a result, the first shots are usually unstable. So, layers deposited under such non-recurrent conditions (with or without pinch) are not comparable. To eliminate this fault, between the anode and the sample the shutter was mounted. The shutter is 6 cm in diameter and it can be moved across the chamber (Fig. 1). The shutter avoids the deposition of any material emitted during the preliminary shots until a good focusing achieved. During experiments, the shutter shielded the Si wafers for the first four shots. Then the shutter was moved near to a wall of the chamber and the sample was exposed to a plasma action.

The nano-layers were deposited in 10 shots at 50, 200 and 1000 mTr. Current and derivative of current were reordered by digital oscilloscope Tektronix 3052. The waveforms of current and its derivative were shown in our earlier paper [6].

The topography of layer was investigated using scanning electron microscopy (SEM). The composition of the layer was investigated using Auger spectroscopy (AES).

3. Results and discussion

The surfaces of some samples are shown in Figs. 2–4. In these figures, it can be observed that the surface is smooth when the deposition process is proceeded at 50 and 1000 mTr of pressure. On the contrary, many nano- and micro-drops are present at the sample surface after deposition at 200 mTr of pressure (Fig. 3). Presence and absence of drops is possible to explain. In the beginning, it should be described how the material from the anode is emitted during the discharge. So, during pinch the electron beam is generated [8]. The electron beam moves in the direction of the anode. Then, as a result of interaction of electron beam with the anode, X-ray and the anode material are emitted. It is obvious that the amount of emission depends on the electron beam intensity. The material emission increases with the electron beam intensity increasing. Intensity of electron beam emission can be changed by gas pressure in reactor chamber [8]. With increasing pressure, the electron beam intensity decreases. Consequently, the material emission decreases.

At 50 mTr of pressure the pinch usually does not appear and is feebly marked. Therefore, the intensity of electron beam was very low and only single atoms or ions were emitted from the anode. For this reason the surface is very smooth. When the pressure increased up to 200 mTr, the pinch always appeared. Since the pressure was relatively low, the electron beam intensity was high. Therefore, not only single ions or atoms were emitted from the end of anode, but also big fragments of the anode were emitted, like clusters composed from several tens of atoms. These clusters moved in the direction of the sample and were

deposited at the sample surface. In this case, many drops were observed at the surface. These suppositions are confirmed by observations of the surface of layer, which was deposited at 1000 mTr of pressure. This sample is smooth, because the electron beam intensity is smaller at 1000 mTr of pressure than at 200 mTr of pressure. So, the electron beam is too small to emit clusters, and only single particles are emitted.

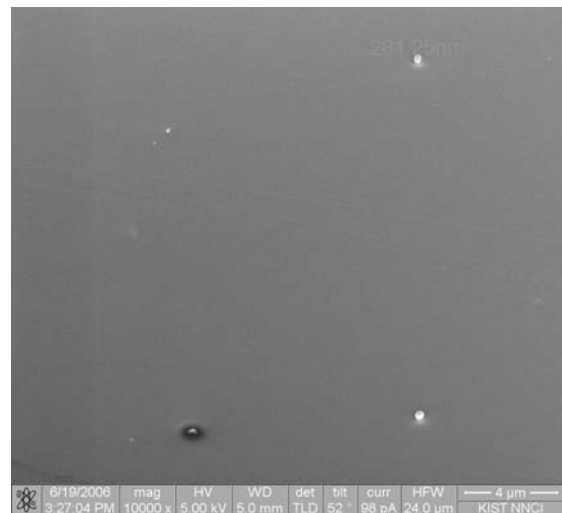


Fig. 2. SEM images for the sample deposited at 50 mTr of pressure of argon-oxygen gas mixture in 10 shots

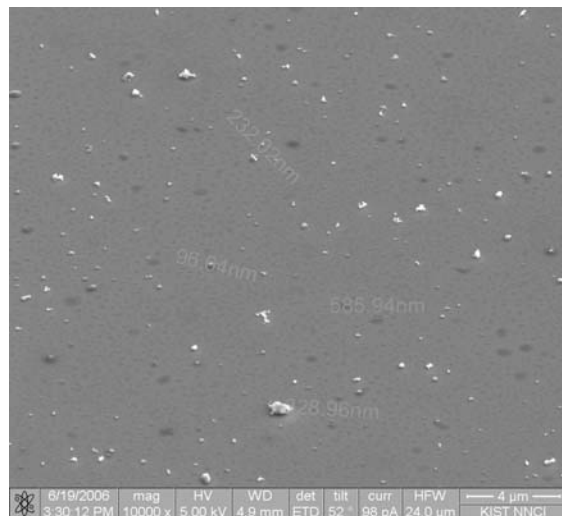


Fig. 3. SEM images for the sample deposited at 200 mTr of pressure of argon-oxygen gas mixture in 10 shots

Now it is clear that to obtain smooth surface the depositing process should be proceeded at low pressure without pinch formation or at high pressure without appearance of a pinch.

In the Figs. 5–7 the depth profiles of the films are shown. The results pointed out that the films were composed of oxygen, chromium, silicon, carbon and copper. The films were free from iron contaminations, which can originate from the cathode.

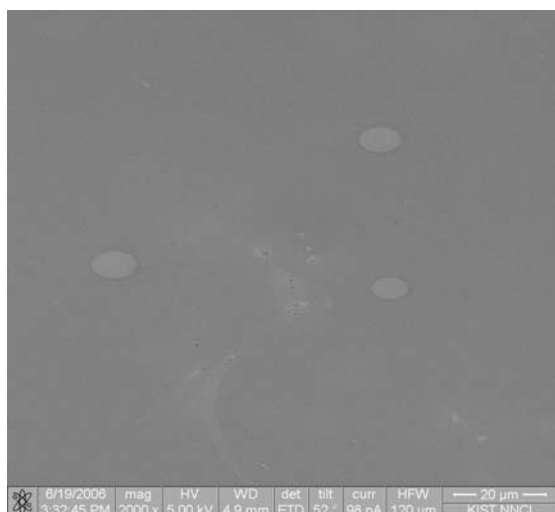


Fig. 4. SEM images for the sample deposited at 1000 mTr of pressure of argon-oxygen gas mixture in 10 shots

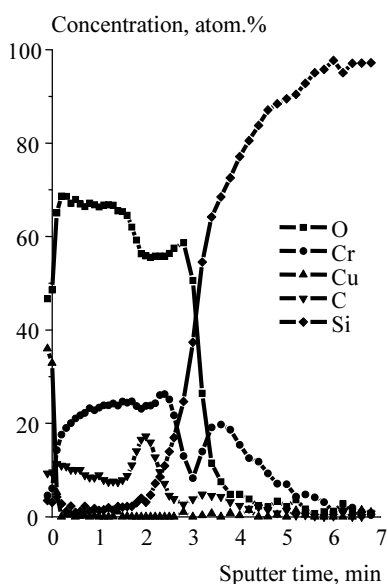


Fig. 5. AES analysis of the sample deposited at 50 mTr of pressure of argon-oxygen gas mixture in 10 shots

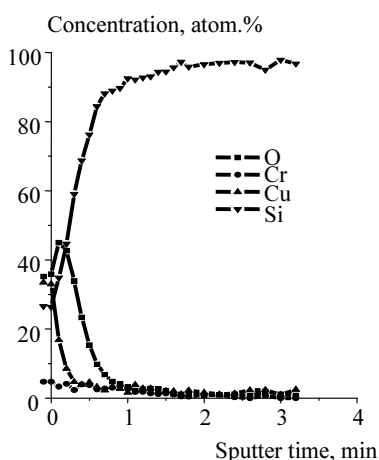


Fig. 6. AES analysis of the sample deposited at 200 mTr of pressure of argon-oxygen gas mixture in 10 shots

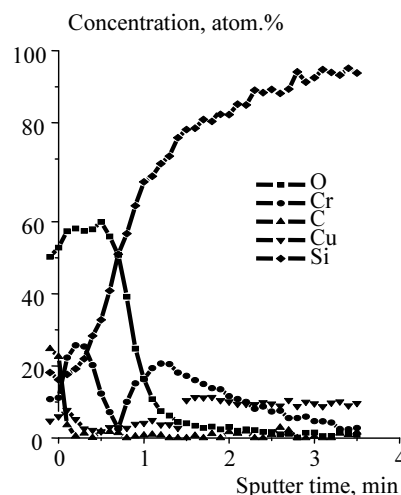


Fig. 7. AES analysis of the sample deposited at 1000 mTr of pressure of argon-oxygen gas mixture in 10 shots

Presence of chromium and oxygen was expected. Chromium is emitted from the anode end. Oxygen is the main component of gas mixture, which fills the chamber and in consequence of surface oxidizing it was introduced to the layer.

Silicon comes from the base material (silicon wafer). It could be mixed with the depositing material during the deposition process or during AES investigations. In both cases, the sample surface was exposed to the action of high-energetic particles. Therefore, some amount of silicon atoms can get into the layer.

The presence of carbon in the layer suggested that a vapor of oil from vacuum pumps was in the vacuum chamber. During our experiments, the oil rotary pump and diffusion pump were used. It means that the pumps should be exchanged for oil-free pumps.

The copper comes from the anode wall or the anode end, as only a central part of the anode end is made of chromium. But nano-layers were free from the iron. It means that the cathode wall is not a source of depositing material. Similar, the wall of the anode should not introduce the copper into nano-layers. It suggested that the copper was emitted from the anode end. It means that the anode construction is significant and its construction decides about the nano-layer composition.

4. Summary and conclusions

Generally, nano-layers can be effectively deposited using the PF device.

Nano-layers contain chromium, oxygen, copper, silicon and carbon. Oil-free vacuum pumps and new type of anode end should be used to eliminate carbon and copper.

The process of nano-layers deposition should be carried out at low pressure without pinch formation or at high pressure with the pinch. Under these conditions, the surface was smooth. Many micro-drops were on the surface when the process was carried out at low pressure with pinch.

References

- [1] E.B. Aurahan and Y. Porath, Nucl. Instrum. Meth. **123**, 5 (1975).
- [2] Y. Kato and S.H. Be, Appl. Phys. Lett. **48**, 686 (1986).
- [3] E.P. Bogolubov, V.D. Bochkov, A.V. Dubrovski, X. Feng, V.A. Gribkov, Y.P. Ivanov, A.I. Isakov, O.N. Krohin, P. Lee, S. Lee, V.Y. Nikulin, A. Serban, P.V. Silin, G.Z. Zhang, V.A. Veretennikov, and L.T. Vekhoreva, Physica Scripta **57**, 488 (1998).
- [4] S. Hussain, M. Shafiq, R. Ahmad, A. Waheed, and M. Zakauallah, Plasma Sources Science and Technology **14**, 61 (2005).
- [5] R.S. Rawat, M.P. Srivastava, S. Tandon, and A. Mansingh, Phys. Rev. **B 47**, 4858 (1993).
- [6] M. Chernyshova, I. Ivanova-Stanik, L. Karpiński, M. Scholz, B. Ulejczyk, I.N. Demchenko, and J.K. Lee, Czechoslovak Journal of Physics **B 56**, 237 (2006).
- [7] A. Lepone, H. Kelly, D. Lamas, and A. Marquez, Applied Surface Science **143**, 124 (1999).
- [8] A. Bernard, H. Bruzzone, P. Choi, H. Chuaqui, V. Gribkov, J. Herrera, K. Hirano, A. Krejčí, S. Lee, C. Luo, F. Mezzetti, M. Sadowski, H. Schmidt, K. Ware, C.S. Wong, and V. Zoita, J. Moscow Phys. Soc. **8**, 93 (1998).